THE JOURNAL OF PHYSICAL CHEMISTRY A

Article

pubs.acs.org/JPCA

Cooperative Effects and Optimal Halogen Bonding Motifs for Self-Assembling Systems

Xin Cindy Yan, Patric Schyman, and William L. Jorgensen*

Department of Chemistry, Yale University, New Haven, Connecticut 06520-8107, United States

ABSTRACT: Halogen bonding, due to its directionality and tunable strength, is being increasingly utilized in self-assembling materials and crystal engineering. Using density functional theory (DFT) and molecular mechanics (OPLS/CM1Ax) calculations, multiply halogen bonded complexes of brominated imidazole and pyridine are investigated along with their potential in construction of self-assembling architectures. Dimers with 1−10 halogen bonds are considered and reveal maximal binding energies of 3−36 kcal/mol. Cooperative (nonadditive) effects are found in complexes that extend both along and perpendicular to the halogen bonding axes, with interaction energies depending on polarization, secondary interactions, and ring spacers. Four structural motifs were identified to yield optimal halogen bonding. For the largest systems, the excellent agreement found between the DFT and OPLS/CM1Ax results supports the utility of the latter approach for analysis and design of self-assembling supramolecular structures.

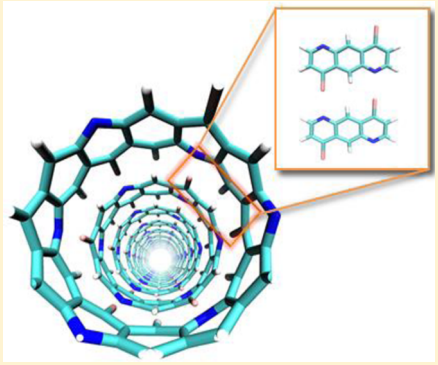

INTRODUCTION

Halogen bonding has emerged in recent years as an effective alternative to hydrogen bonding in directing the formation of self-assembling architectures, with fruitful applications in many chemical[1−3] and biological[4−6] systems. Halogen bonding is an electrostatically driven noncovalent interaction between a halogen atom in one molecule and a lone-pair (n) or π-electron donor in another.[7] The electron-withdrawing effect of groups covalently bound to a halogen atom depletes the electron density in the n_σ orbital to yield an electropositive "σ-hole".[8] Halogen bonding serves as an ideal cohesive force in self-assembling systems due to its linear directionality,[9,10] tunable bonding strength,[11−13] and stability in hydrophobic environments.[4] In addition to attractive intermolecular forces, self-assembling processes may be aided via cooperative effects,[14,15] i.e., nonadditive enhancement from polarization and charge transfer. The existence of cooperativity in halogen bonding has been identified in previous crystallographic[16] and theoretical studies[17−20] covering molecular complexes with varied structures and strengths.

The present computational study expands upon previous efforts to quantitatively examine cooperative effects and optimal motifs for linear and multiply halogen bonded systems and to consider their potential in the construction of self-assembling architectures. By performing density functional theory (DFT) calculations, enhanced understanding is sought on the nature of cooperativity through geometrical, energetic, and natural bonding orbital (NBO) analyses.[21] Factors are considered that could influence interaction strength such as polarization, secondary interactions, and spacing between halogen bonds. Recently, modeling of halogen bonding interactions in supramolecular systems has been facilitated in force fields by representing the σ-hole as a partial positive point charge attached to the halogen atom.[22,23] Carter et al.[24] also redesigned a force field for halogen bonds by including angular dependency into the standard Lennard-Jones potential. In the present work, model systems are considered and then extended to construct cylindrical complexes analogous to carbon nanotubes (CNTs).

RESULTS

Cooperativity in Linear Chains. The initial focus was on 4-bromopyridine and 1-bromo-1*H*-imidazole as prototypical building blocks for construction of larger, self-assembling systems. The first issue was to evaluate the structures, interaction strengths, and cooperativity for linear oligomers, namely, (4-bromopyridine)$_n$ (**1**) and (1-bromo-1*H*-imidazole)$_n$ (**2**) with n = 1−6, as shown in Figure 1 for n = 4. As described

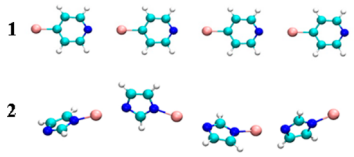

Figure 1. Optimized geometries of linear chains for tetramers of 4-bromopyridine (**1**) and 1-bromo-1*H*-imidazole (**2**).

in Computational Methods, DFT calculations were carried at the M06-2X/6-31+G(d,p)-LanL2DZdp-PP level with counterpoise corrections using geometries optimized with the ωB97X functional and the same basis set.

As reported in Table 1, the calculated average halogen-bond lengths decline and binding energies strengthen steadily with

Received: February 12, 2014
Revised: March 27, 2014
Published: March 29, 2014

Table 1. Average Halogen Bond Lengths, $\langle R_{XB}\rangle$, Binding Energies, $-\Delta E_{bind}$, Average Halogen Bonding Energies, $\langle -E_{XB}\rangle$, and Average Cooperative Energies, $\langle E_{coop}\rangle$ for the Linear Oligomers[a]

n	$\langle R_{XB}\rangle$	$-\Delta E_{bind}$	$\langle -E_{XB}\rangle$>	$\langle E_{coop}\rangle$
	Compound **1**, (4-Bromopyridine)$_n$			
2	3.051	2.94 (2.71)[c]	2.94	
3	3.039 (−0.4%)[b]	6.02 (5.54)	3.01 (2.6%)[b]	−0.15
4	3.034 (−0.5%)	9.15 (8.41)	3.05 (3.8%)	−0.17
5	3.033 (−0.6%)	12.28 (11.07)	3.07 (4.6%)	−0.18
6	3.031 (−0.7%)	15.42 (13.91)	3.08 (5.0%)	−0.19
	Compound **2**, (1-Bromo-1*H*-imidazole)$_n$			
2	2.674	8.31 (7.55)	8.31	
3	2.608 (−2.4%)	18.27 (16.73)	9.13 (9.9%)	−1.64
4	2.567 (−4.0%)	28.97 (26.44)	9.66 (16.2%)	−2.02
5	2.535 (−5.2%)	40.08 (36.77)	10.02 (20.6%)	−2.28
6	2.514 (−6.0%)	51.48 (47.33)	10.30 (23.9%)	−2.48

[a]Distances in angstroms; energies in kilocalories per mole. [b]Percentage change compared to the dimer. [c]The energy difference between the optimized complex and separated monomers including zero-point energy corrections.

growing oligomer size. The average halogen-bond strength increases for the 4-bromopyridine case from 2.94 to 3.08 kcal/mol for n = 2−6. The interactions and cooperative effects for the imidazole case are notably stronger, advancing from 8.31 kcal/mol for the dimer to 10.30 kcal/mol for the hexamer. The halogen bonds are also significantly shorter with N···Br separations near 2.5 Å for **2** versus 3.0 Å for **1**. The much stronger halogen bonds for **2** are due to the nitrogen atom being covalently bound to bromine, which simultaneously enhances electron withdrawal from bromine by induction and electron donation to the Lewis basic nitrogen by resonance. Most of the linear chains of both compounds exhibit nonuniform sequential arrangements, with shorter halogen-bond distances in the middle and longer ones toward the ends of the chains. This geometric characteristic has also been found in hydrogen-bonded linear chains.[25,26] As also shown in Table 1 (column 3), including zero-point energy (ZPE) corrections decreases the estimated strength of the halogen bonds uniformly by about 10%.

Cooperative effects are apparent in the increasing average strengths of the halogen bonds. Further quantification comes from evaluating the average cooperative energy, E_{coop}, according to eq 1 for oligomers of sizes greater than 2.[27] As shown in Table 1, the negative values for E_{coop} confirm the existence of cooperative effects in all cases, and they increase in magnitude as the chains grow.

$$E_{coop} = [\Delta E_{bind}(\text{cluster}) - (n-1)\Delta E_{bind}(\text{dimer})]/(n-2) \quad (1)$$

A many-body analysis was also carried out using the standard partition scheme of Hankins et al.[28] for the trimers and tetramers. This requires calculations for each constituent n-mer to yield the total interaction energy as a sum of contributions from two-, three-, and four-body interactions. The results in Table 2 indicate that while the two-body interactions make the dominant contributions to the binding energies, the three-body terms are substantial and increase significantly in going from the trimers to tetramers. However, the four-body terms are negligible, as found in a previous many-body analysis of hydrogen-bonded HCN chains.[29]

Table 2. Many-Body Decomposition of the Interaction Energy for the Trimers and Tetramers[a]

n	two-body	three-body	four-body
	Compound **1**, (4-Bromopyridine)$_n$		
3	−5.94 (97.6%)[b]	−0.15 (2.4%)	
4	−8.93 (96.4%)	−0.32 (3.4%)	−0.02 (0.2%)
	Compound **2**, (1-Bromo-1*H*-imidazole)$_n$		
3	−17.45 (91.2%)	−1.68 (8.8%)	
4	−26.29 (85.7%)	−4.05 (13.2%)	−0.34 (1.1%)

[a]Energies in kilocalories per mole including counterpoise corrections. [b]Percentage of the total interaction energy.

To further characterize the cooperative effects, the investigations considered the changes in dipole moment and intermolecular orbital interactions via NBO analysis. The average dipole moment per molecule ($\langle\mu\rangle$) and the cooperative dipole moment ($\langle\mu_{coop}\rangle$, defined analogously to the cooperative energy, increase for addition of each monomer (Table 3). The

Table 3. Calculated Average Dipole Moments, $\langle\mu\rangle$, Cooperative Dipole Moments, $\langle\mu_{coop}\rangle$, Average $n_N \rightarrow \sigma^*_{C-Br}$ Charge Transfer, $\langle q_{CT}\rangle$, and Average Delocalization Energies, $\langle E^{(2)}\rangle$[a]

n	$\langle\mu\rangle$	$\langle\mu_{coop}\rangle$	$\langle q_{CT}\rangle$	$\langle E^{(2)}\rangle$
	Compound **1**, (4-Bromopyridine)$_n$			
2	1.33	1.20	0.0077	2.98
3	1.59	1.29	0.0083	3.12
4	1.73	1.34	0.0085	3.17
5	1.82	1.37	0.0085	3.19
6	1.88	1.38	0.0086	3.24
	Compound **2**, (1-Bromo-1*H*-imidazole)$_n$			
2	4.15	2.62	0.0341	12.53
3	4.86	3.03	0.0450	15.98
4	5.44	3.47	0.0526	18.77
5	5.84	3.75	0.0601	21.26
6	6.17	4.00	0.0664	23.22

[a]Dipole moments in Debyes; transferred charges in e; energies in kilocalories per mole.

calculated average intermolecular charge transfer ($\langle q_{CT}\rangle$) and delocalization energies ($\langle\Delta E^{(2)}\rangle$) associated with the lone pair on the nitrogen atoms (n_N) and antibonding orbitals of the C−Br bonds (σ^*_{C-Br}) are also found to increase with the size of the oligomers in Table 3. Moreover, Figure 2 illustrates that the average binding energy correlates linearly with average dipole moment (correlation coefficient = 0.998 and 0.994) and transferred charge (correlation coefficient = 0.954 and 0.981). Overall, the present results support the consensus view that polarization is a major source of the cooperativity in linear halogen-bonded systems.[18,19]

Cooperativity in Multiply Halogen Bonded Systems. While previous studies have focused on the cooperativity in linear systems, the cooperativity in multiply halogen bonded systems was also explored here for a variety of haloazines. The goals are to identify the factors that influence halogen-bond strengths and to determine optimal halogen-bonding motifs for potential use in self-assembly of large systems. As shown in Figure 3 and Table 4, results were obtained for the singly, doubly, and triply halogen bonded complexes **3a**−**3c**. These cases illustrate alternation of the donor and acceptor sites at the interface. The average length of the halogen bonds increases

dx.doi.org/10.1021/jp501553j | J. Phys. Chem. A 2014, 118, 2820−2826

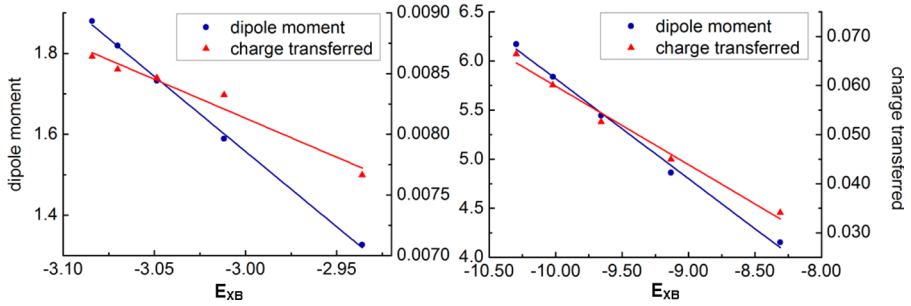

Figure 2. Correlations of the average halogen bonding energy ($\langle E_{XB} \rangle$, kcal/mol) with the average dipole moment (debyes) and average amount of charge transferred (e) for linear oligomers of (4-bromopyridine)$_{2-6}$ on the left and (1-bromo-1*H*-imidazole)$_{2-6}$ on the right.

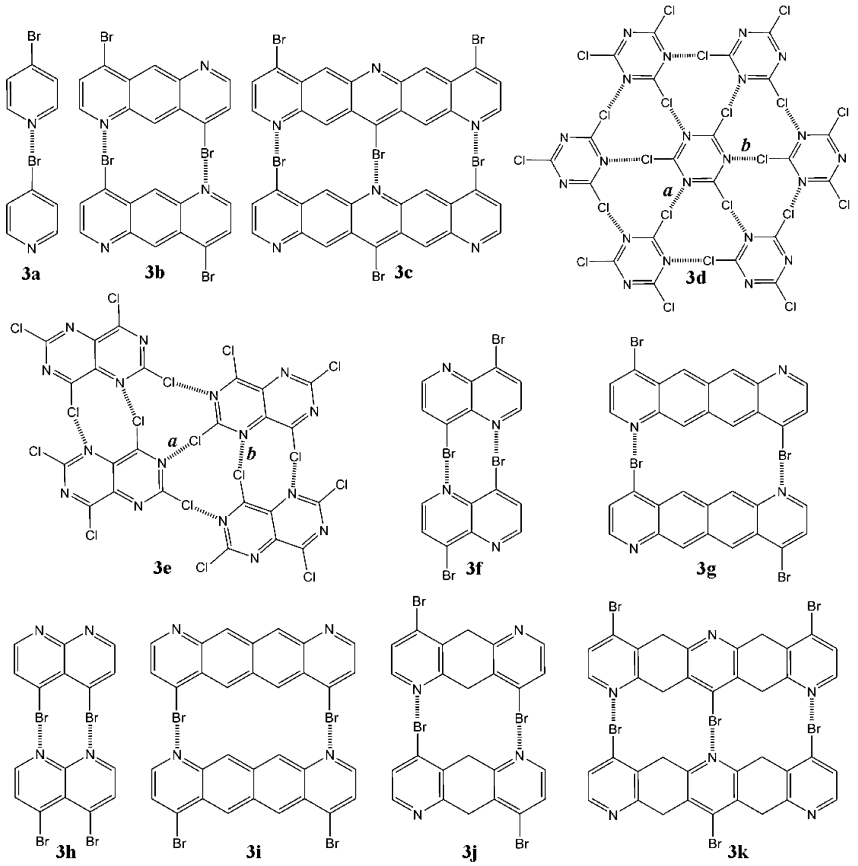

Figure 3. Halogen-bonded complexes for haloazines.

slightly along this series, which likely reflects the unfavorable H···H repulsions across the interfaces for **3b** and **3c**. Nevertheless, the average strength increases from 2.94 to 3.39 kcal/mol. Notably, the total binding energy for **3c** is ca. 10 kcal/mol, which is stronger by 1 kcal/mol than for the tetramer of **1**, also featuring three halogen bonds. Thus, the cooperative effect is somewhat greater for extension of the halogen bonding system laterally rather than in a linear, head-to-tail manner.

Related systems that incorporate extensive two-dimensional networks of nitrogen−chlorine halogen bonds have been reported in crystallographic studies.[30−34] In the present work, two of the azaaromatic chlorides were revisited: cyanuric trichloride (**3d**) and 2,4,6,8-tetrachloropyrimido[5,4-*d*]-pyrimidine (**3e**). The dimer and heptamer of **3d** and the dimer and tetramer for **3e** were optimized. As shown in Table 4, the DFT results for the halogen-bond lengths for the oligomers of **3d** and **3e** are in excellent agreement with the findings from the X-ray crystallography.[34] However, compared to the bromoazines, the DFT results reveal that the halogen bonds for **3d** and **3e** are significantly weaker with average strengths of 1.5−1.9 kcal/mol. Similarly, in our prior study of the complexes of bromobenzene and chlorobenzene with pyridine, binding energies of 2.7 and 1.9 kcal/mol were obtained.[22] Though the halogen bonds for **3d** and **3e** are weak, they clearly contribute to the packing and self-assembly reflected in the crystal structures.[34] Stronger halogen bonding interactions can be expected to lead to more robust self-assembling materials.

Continuing in Figure 3, **3f** and **3g** remove or add a benzene spacer to **3b**. The binding energy for **3f** is significantly weaker at 3.37 kcal/mol owing to the repulsion between the central bromine atoms; the monomers shift laterally such that the C−Br···N angles are 164° rather than the optimal 180° for halogen bonds. However, the additional spacer in **3g** has little impact

dx.doi.org/10.1021/jp501553j | *J. Phys. Chem. A* 2014, 118, 2820−2826

Table 4. Average Halogen Bond Lengths, $\langle R_{XB} \rangle$, Binding Energies, $-\Delta E_{bind}$, Average Halogen Bonding Energies, $\langle -E_{XB} \rangle$, and Average Cooperative Energies, $\langle E_{coop} \rangle$ in Multiply Halogen Bonded Systems[a]

complex	$\langle R_{XB} \rangle$	$-\Delta E_{bind}$	$\langle -E_{XB} \rangle$	$\langle E_{coop} \rangle$
3a	3.051	2.94 (2.71)[c]	2.94	
3b	3.092	6.60 (5.77)	3.30 (12.5%)[d]	−0.73
3c	3.093	10.18 (9.68)	3.39 (15.6%)	−0.69
3d (dimer)	3.115	1.76	1.76	
3d (heptamer)				
(a)	3.108 (3.100)[b]	22.18	1.85	−0.09
(b)	3.111 (3.116)[b]			
3e (dimer)	3.341	3.00	1.50	
3e (tetramer)				
(a)	3.172 (3.207)[b]	10.81	1.54	n.d.[e]
(b)	3.320 (3.332)[b]			
3f	3.376	3.37 (3.10)	1.68 (−42.7%)	2.51
3g	3.098	6.27 (5.82)	3.13 (6.7%)	−0.39
3h	3.231	3.55 (3.10)	1.77 (−39.6%)	2.33
3i	3.098	5.60 (5.19)	2.80 (−4.7%)	0.28
3j	3.104	7.16 (7.00)	3.58 (21.9%)	−1.28
3k	3.085	11.34 (10.65)	3.78 (28.7%)	−1.26

[a]Distances in Ångstroms; energies in kilocalories per mole. [b]Halogen bond lengths in the crystal structures from ref 32. [c]Including zero-point energy corrections. [d]Percentage increase compared to **3a**. [e]Not determined.

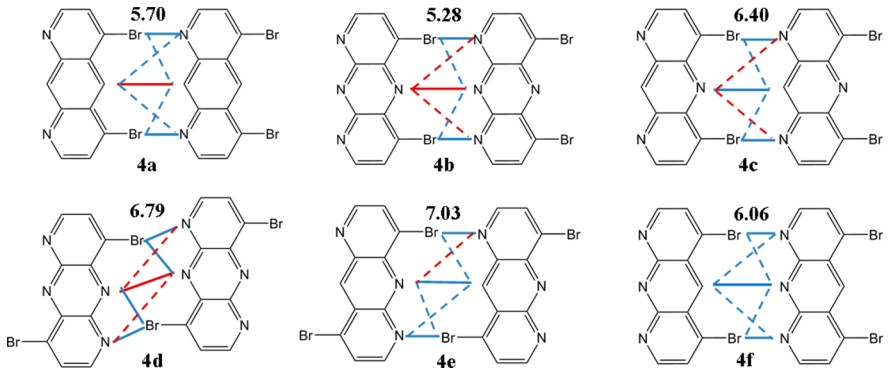

Figure 4. Six alternative doubly halogen bonded complexes with their computed binding energies $-\Delta E_{bind}$ (kcal/mol) from M06-2X/6-31+G(d,p)-LanL2DZdp-PP calculations. Primary interactions are indicated with solid lines and secondary ones are shown with dashed lines. Blue and red colors tentatively assign attractive and repulsive interactions, respectively.

yielding an interaction energy nearly the same as that for **3b**. Complexes **3h** and **3i** are isomeric with **3f** and **3g**; however, both donors and both acceptors are now on the same side of the interface. For hydrogen-bonded systems, this arrangement can lead to stronger binding owing to the favorable secondary electrostatic interactions.[35] However, in **3h** the repulsion between the bromines causes them to bend away from each other with C−C−Br angles of 125° and C−Br···N angles of 162°, which leads to weak binding of only 3.55 kcal/mol. The problem is relieved for **3i**, though its binding energy of 5.60 kcal/mol is about 0.7 kcal/mol weaker than for **3g**. There are small structural differences in this case; the halogen bonds are more linear for **3g** than **3i** with C−Br···N angles of 178° for **3g** and 173° for **3i**. Finally, **3j** and **3k** explore replacement of the benzene rings in **3b** and **3c** with cyclohexyl spacers. The N···Br halogen bond lengths are constant at 3.09−3.10 Å; however, the partially saturated systems exhibit stronger attraction with binding energies of 7.16 and 11.34 kcal/mol for **3j** and **3k**. The increased attraction can be attributed to reduced H···H repulsion across the interfaces. For the unsaturated cases such as **3b**, **3c**, and **3g**, the shortest interannular H···H contacts are 2.8−2.9 Å, while they are 3.4−3.5 Å for the partially saturated **3j** and **3k**.

Thus, for the motifs in Figure 3, the strongest average halogen bond strengths occur when the donor and acceptor sites alternate on each side of the interface and when there is a spacer ring between the 4-bromopyridine subunits as in **3b** and **3j**. Significant cooperative effects are apparent with the average N···Br halogen bond strength climbing from 2.94 kcal/mol in the reference dimer **3a** to 3.39 kcal/mol in **3c** and to 3.78 kcal/mol in **3k**. This analysis assigns all of the net interaction to the halogen bonds, which is an oversimplification since there are at least varying steric effects associated with the H···H interactions at the interface. However, the results establish that multiply halogen bonded interfaces can be constructed where the net interaction is more attractive than from the sum of the individual halogen bonds.

Further Consideration of Secondary Interactions and Spacers. In view of the possible influence of secondary electrostatic interactions on complexation,[35] six additional dimers related to **3b** were considered (Figure 4 and Table 5). Each complex formally has two N···Br halogen bonds; however, the interface has been modified by the arrangement of the

dx.doi.org/10.1021/jp501553j | J. Phys. Chem. A 2014, 118, 2820−2826

Table 5. Average Halogen Bond Lengths, $\langle R_{XB}\rangle$, Binding Energies, $-\Delta E_{bind}$, Average Halogen Bonding Energies, $\langle -E_{XB}\rangle$, and Average Cooperative Energies, $\langle E_{coop}\rangle$ in Doubly Halogen Bonded Systems[a]

complex	$\langle R_{XB}\rangle$	$-\Delta E_{bind}$	$\langle -E_{XB}\rangle$	$\langle E_{coop}\rangle$
3b	3.092	6.60 (5.77)[b]	3.30	−0.73
4a	3.114	5.70 (5.30)	2.85	0.17
4b	3.085	5.28 (4.87)	2.64	0.59
4c	3.076	6.40 (6.01)	3.20	−0.53
4d	3.114	6.79 (6.39)	3.40	−0.92
4e	3.066	7.03 (6.45)	3.52	−1.16
4f	3.093	6.06 (5.70)	3.03	−0.19

[a]Distances in Ångstroms; energies in kilocalories per mole. [b]Including zero-point energy corrections.

donors and acceptors or by modification of the central ring as benzene, pyridine, or pyrazine. Compound **4a** is the isomer of **3b** with both donors on one side of the interface and both acceptors on the other. As with **3g** and **3i**, the preference is for the alternating arrangement in **3b** over the parallel one in **4a** by nearly 1 kcal/mol. Compound **4b** replaces the central benzene ring of **4a** with pyrazine. The introduction of the interfacial N···N repulsion does weaken the binding to 5.28 kcal/mol. Compound **4c** is then the analogue with the central ring as pyridine. This replaces the N···N repulsion with an N···H attraction, and the binding is enhanced to 6.40 kcal/mol.

Complexes **4d** and **4e** are the analogues of **3b** with the pyrazine and pyridine spacers; they are also isomers of **4b** and **4c** with the donor and acceptor arrangement returned to alternating. These complexes both show some enhancement of the binding energy to 6.79 and 7.03 kcal/mol. For **4d** the interannular N···N repulsion is diminished by a lateral shift such that the N···Br halogen bonds become somewhat bifurcated.[36,37] The outer C−Br···N angle is 173° in **4d**, while the inner one is 148°, and the central N···N distance is 5.0 Å. In **4e**, the halogen bonds are nearly linear (178°) and the central C−H···N interaction is electrostatically attractive.

Compound **4f** is the final possibility in this series; it is the isomer of **4c** with the three nitrogen atoms on one edge. The binding weakens to 6.06 kcal/mol, which suggests that the basicity of the nitrogens in **4f** is lessened by their proximity. There is also a geometrical effect; the collection of short C−N bonds induces slight concave curvature to the nitrogen-containing edges in **4f** that splays out the opposite bromine-containing edges. In turn, this adversely affects the linearity of the halogen bonds in **4f** with C−Br···N angles of 171° vs 178° in **4c**.

These results establish that **3b**, **3j**, **4d**, and **4e** represent the motifs with the most attractive interactions. They feature 4-bromopyridine units with edges of alternating donor and acceptor sites separated by a monocyclic spacer. They can all be extended to potentially yield sheetlike structures in the solid state and a foundation for construction of other self-assembling materials.

Application to Self-Assembly in Three Dimensions. The possible utility of the **3b** motif for constructing tubelike structures that could self-assemble was considered. Cylindrical belts were generated with alternating 4-bromopyridine and benzene rings and alternating up/down arrangement of the bromopyridines. Dimers of the belts with six (**5a**), eight (**5b**), and ten (**5c**) repeats can form six, eight, and ten halogen bonds at each interface (Figure 5). The dimers were modeled with DFT and molecular mechanics calculations. For the latter, the fixed-charge force field, OPLS/CM1Ax, was used as well as the version that includes polarization via induced dipoles on non-hydrogen atoms, OPLS/CM1AxP.[22,38,39] Both force fields incorporate partial positive charges (X-sites) to represent the σ-holes on chlorine, bromine, and iodine atoms.[22] The energetic results for **5a**, **5b**, and **5c** are summarized in Table 6. In view of the increasing system sizes, two alternatives for the DFT method and basis sets were needed. As noted in Table 6, both procedures gave similar results for **5a**. The geometry optimizations for **5b** and **5c** used the smaller 6-31G(d)-LanL2DZdp-PP basis set with BLYP, and the isolated monomer geometry was taken to be the same as in the optimized dimer.

Table 6. Energetic Results (kcal/mol) for Halogen-Bonded Dimers Using OPLS/CM1Ax Force Fields and DFT Calculations

	OPLS/CM1Ax		OPLS/CM1AxP		DFT	
complex	$-\Delta E_{bind}$	$\langle -E_{XB}\rangle$	$-\Delta E_{bind}$	$\langle -E_{XB}\rangle$	$-\Delta E_{bind}$	$\langle -E_{XB}\rangle$
3b	6.07	3.04	6.61	3.30	6.60[a]	3.30
3c	9.50	3.17	10.35	3.45	10.18[a]	3.39
5a	23.03	3.84	25.33	4.22	19.46[b]	3.24
					20.05[c]	3.34
5b	28.59	3.57	31.42	3.93	27.23[c]	3.40
5c	35.66	3.57	39.31	3.93	34.55[c]	3.46

[a]Using M06-2x//ωB97X with the 6-31+G(d,p)-LanL2DZdp-PP basis set. [b]Using M06-2x//B97-1 with the 6-31G(d,p)-LanL2DZdp-PP basis set. [c]Using M06L/6-31G(d,p)-LanL2DZdp-PP//BLYP/6-31G(d)-LanL2DZdp-PP.

For **3b** and **3c** as references, the binding energies from the force field calculations are found to be in near perfect agreement with the M06-2X results. This is not unexpected since OPLS/CM1Ax was parametrized to reproduce halogen-bonding results from high-end *ab initio* calculations, specifically, MP2(FULL)/aug-cc-pVDZ(-PP).[22] Addition of polarization strengthens the binding by about 10%. The close agreement

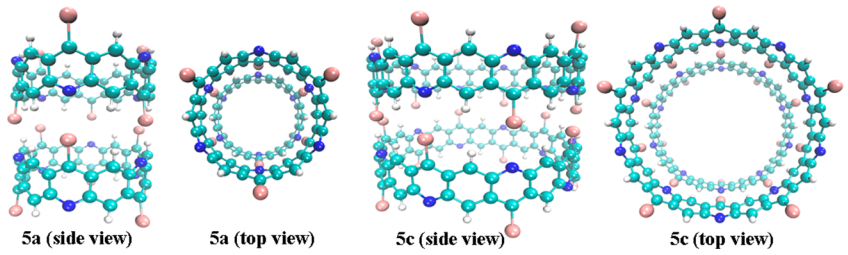

Figure 5. Supramolecular tubes can be assembled from cylindrical belts using six (**5a**) or ten (**5c**) halogen bonds at each interface.

dx.doi.org/10.1021/jp501553j | J. Phys. Chem. A 2014, 118, 2820−2826

extends to **5a** − **5c** where the best accord is found between the nonpolarizable OPLS/CM1Ax and DFT results. As noted previously, the CM1A charges include the intramolecular electronic polarization for the monomers, and the intermolecular polarization is generally only essential for modeling interactions with small ions.[38]

Notably, along the **5a**−**5c** series the binding intensifies from 20 to 27 to 35 kcal/mol. There is also a gradual increase in the average halogen bond strength from 3.24 to 3.46 kcal/mol according to the DFT calculations. This cooperative effect is not mirrored in the force field results which yield the same average halogen bond strength for the two larger systems. The strong binding for **5a**−**5c** indicates that the halogen bonding motifs in **3b**, **3j**, **4d**, and **4e** could be used as the cohesive elements to build a wide range of interesting supramolecular systems and nanomaterials. Furthermore, the excellent accord between the DFT and OPLS/CM1Ax results supports the use of OPLS/CM1Ax as a computationally efficient means for modeling such systems.

CONCLUSION

The present study addressed halogen binding strengths and cooperativity in linear and multiply halogen bonded systems. For the linear chains **1** and **2**, cooperative effects progressively strengthen the halogen bonds with the addition of each monomer. The cooperativity is largely a polarization effect, as supported by the close correlations of the cooperative dipole moments and amounts of charge transferred with the interaction energies. For multiply halogen bonded complexes such as **3a**−**3c**, the average halogen bond strength was also found to increase with increasing numbers of halogen bonds. Four motifs, **3b**, **3j**, **4d**, and **4e**, emerged as having particularly strong halogen bonding and symmetries that allow their elaboration to yield large periodic systems. This notion was further explored with the demonstration that molecular belts based on **3b** could be constructed that should self-assemble into nanotubes. Furthermore, the OPLS/CM1Ax force field was confirmed to accurately predict the interaction energies for halogen-bonded systems as large as the belt dimers **5a**−**5c**.

COMPUTATIONAL METHODS

Geometry optimizations were performed with the ωB97X[40,41] functional using the Gaussian 09 program.[42] The 6-31+G(d,p) basis set was employed for all atoms with the exception of bromine, for which the LanL2DZdp-PP basis set with pseudopotentials was used.[43] Vibrational frequency calculations were carried out at the same level to confirm that the optimized structures were true minima. Binding energies were obtained by single-point energy calculations with the M06-2X or M06L functional using the same basis set as the geometry optimization,[44,45] and with basis set superposition error (BSSE) removed via the Boys−Bernardi counterpoise (CP) method.[46] The accuracy of the results from such computations has been supported by numerous benchmark studies.[22,41,44,45,47] Natural bond orbital (NBO) analysis was performed with Gaussian 09 following standard procedures.[48]

Geometry optimizations were also performed using molecular mechanics as implemented in the BOSS 4.9 software.[49] The OPLS/CM1Ax force field, which features 1.14*CM1A partial atomic charges[50] with extra point charges (X-sites) representing the σ-hole for halogen atoms, was used. The effects of inclusion of intermolecular polarization with inducible dipoles were considered with the OPLS/CM1AxP force field.[38,39] The polarizabilities, α, for carbon, nitrogen, and bromine were assigned as 1.0, 1.5, and 2.0 Å^3.

AUTHOR INFORMATION

Corresponding Author

*E-mail: william.jorgensen@yale.edu.

Notes

The authors declare no competing financial interests.

ACKNOWLEDGMENTS

Gratitude is expressed to National Institutes of Health (Grant GM32136) for support of this work. This work was supported in part by the facilities and staff of the Yale University Faculty of Arts and Sciences High Performance Computing Center.

REFERENCES

(1) Meyer, F.; Dubois, P. Halogen Bonding at Work: Recent Applications in Synthetic Chemistry and Materials Science. *CrystEngComm* **2013**, *15*, 3058−3071.

(2) Xu, J. W.; Liu, X. M.; Lin, T. T.; Huang, J. C.; He, C. B. Synthesis and Self-Assembly of Difunctional Halogen-Bonding Molecules: A New Family of Supramolecular Liquid-Crystalline Polymers. *Macromolecules* **2005**, *38*, 3554−3557.

(3) Saccone, M.; Cavallo, G.; MetrangolFo, P.; Pace, A.; Pibiri, I.; Pilati, T.; Resnati, G.; Terraneo, G. Halogen Bond Directionality Translates Tecton Geometry into Self-Assembled Architecture Geometry. *CrystEngComm* **2013**, *15*, 3102−3105.

(4) Voth, A. R.; Hays, F. A.; Ho, P. S. Directing Macromolecular Conformation through Halogen Bonds. *Proc. Natl. Acad. Sci. U. S. A.* **2007**, *104*, 6188−6193.

(5) Voth, A. R.; Khuu, P.; Oishi, K.; Ho, P. S. Halogen Bonds as Orthogonal Molecular Interactions to Hydrogen Bonds. *Nat. Chem.* **2009**, *1*, 74−79.

(6) Lu, Y.; Shi, T.; Wang, Y.; Yang, H.; Yan, X.; Luo, X.; Jiang, H.; Zhu, W. Halogen Bonding: A Novel Interaction for Rational Drug Design? *J. Med. Chem.* **2009**, *52*, 2854−2862.

(7) Politzer, P.; Murray, J. S.; Clark, T. Halogen Bonding: An Electrostatically-Driven Highly Directional Noncovalent Interaction. *Phys. Chem. Chem. Phys.* **2010**, *12*, 7748−7757.

(8) Clark, T.; Hennemann, M.; Murray, J. S.; Politzer, P. Halogen Bonding: the Sigma-Hole. *J. Mol. Model.* **2007**, *13*, 291−296.

(9) Ramasubbu, N.; Parthasarathy, R.; Murrayrust, P. Angular Preferences of Intermolecular Forces around Halogen Centers—Preferred Directions of Approach of Electrophiles and Nucleophiles around the Carbon Halogen Bond. *J. Am. Chem. Soc.* **1986**, *108*, 4308−4314.

(10) Lommerse, J. P. M.; Stone, A. J.; Taylor, R.; Allen, F. H. The Nature and Geometry of Intermolecular Interactions Between Halogens and Oxygen or Nitrogen. *J. Am. Chem. Soc.* **1996**, *118*, 3108−3116.

(11) Metrangolo, P.; Meyer, F.; Pilati, T.; Resnati, G.; Terraneo, G. Halogen Bonding in Supramolecular Chemistry. *Angew. Chem., Int. Ed.* **2008**, *47*, 6114−6127.

(12) Fontana, F.; Forni, A.; Metrangolo, P.; Panzeri, W.; Pilatti, T.; Resnati, G. Perfluorocarbon-Hydrocarbon Discrete Intermolecular Aggregates: An Exceptionally Short N···I Contact. *Supramol. Chem.* **2002**, *14*, 47−55.

(13) Metrangolo, P.; Neukirch, H.; Pilati, T.; Resnati, G. Halogen Bonding Based Recognition Processes: A World Parallel to Hydrogen Bonding. *Acc. Chem. Res.* **2005**, *38*, 386−395.

(14) Ercolani, G. Assessment of Cooperativity in Self-Assembly. *J. Am. Chem. Soc.* **2003**, *125*, 16097−16103.

(15) Alkorta, I.; Blanco, F.; Deya, P. M.; Elguero, J.; Estarellas, C.; Frontera, A.; Quinonero, D. Cooperativity in Multiple Unusual Weak Bonds. *Theor. Chem. Acc.* **2010**, *126*, 1−14.

(16) Bilewicz, E.; Rybarczyk-Pirek, A. J.; Dubis, A. T.; Grabowski, S. J. Halogen Bonding in Crystal Structure of 1-Methylpyrrol-2-yl Trichloromethyl Ketone. *J. Mol. Struct.* **2007**, *829*, 208−211.
(17) Grabowski, S. J.; Bilewicz, E. Cooperativity Halogen Bonding Effect—*Ab Initio* Calculations on $H_2CO\cdots(ClF)_n$ Complexes. *Chem. Phys. Lett.* **2006**, *427*, 51−55.
(18) Solimannejad, M.; Malekani, M.; Alkorta, I. Substituent Effects on the Cooperativity of Halogen Bonding. *J. Phys. Chem. A* **2013**, *117*, 5551−5557.
(19) Alkorta, I.; Blanco, F.; Elguero, J. A Computational Study of the Cooperativity in Clusters of Interhalogen Derivatives. *Struct. Chem.* **2009**, *20*, 63−71.
(20) Esrafili, M. D.; Hadipour, N. L. Characteristics and Nature of Halogen Bonds in Linear Clusters of NCX (X = Cl, and Br): An *ab Initio*, NBO and QTAIM Study. *Mol. Phys.* **2011**, *109*, 2451−2460.
(21) Reed, A. E.; Curtiss, L. A.; Weinhold, F. Intermolecular Interactions from A Natural Bond Orbital, Donor−Acceptor Viewpoint. *Chem. Rev.* **1988**, *88*, 899−926.
(22) Jorgensen, W. L.; Schyman, P. Treatment of Halogen Bonding in the OPLS-AA Force Field: Application to Potent Anti-HIV Agents. *J. Chem. Theory Comput.* **2012**, *8*, 3895−3901.
(23) Ibrahim, M. A. A. AMBER Empirical Potential Describes the Geometry and Energy of Noncovalent Halogen Interactions Better than Advanced Semiempirical Quantum Mechanical Method PM6-DH2X. *J. Phys. Chem. B* **2012**, *116*, 3659−3669.
(24) Carter, M.; Rappe, A. K.; Ho, P. S. Scalable Anisotropic Shape and Electrostatic Models for Biological Bromine Halogen Bonds. *J. Chem. Theory Comput.* **2012**, *8*, 2461−2473.
(25) Chen, Y. F.; Dannenberg, J. J. Cooperative 4-Pyridone H-Bonds with Extraordinary Stability. A DFT Molecular Orbital Study. *J. Am. Chem. Soc.* **2006**, *128*, 8100−8101.
(26) Alkorta, I.; Blanco, F.; Elguero, J. Dihydrogen Bond Cooperativity in Aza-borane Derivatives. *J. Phys. Chem. A* **2010**, *114*, 8457−8462.
(27) Scheiner, S. *Hydrogen Bonding: A Theoretical Perspective*; Oxford University Press: New York, 1997.
(28) Hankins, D.; Moskowitz, J. W.; Stillinger, F. H. Water Molecule Interactions. *J. Chem. Phys.* **1970**, *53*, 4544−4554.
(29) Rivelino, R.; Chaudhuri, P.; Canuto, S. Quantifying Multiple-Body Interaction Terms in H-Bonded HCN Chains with Many-Body Perturbation/Coupled-Cluster Theories. *J. Chem. Phys.* **2003**, *118*, 10593−10601.
(30) Lonsdale, K.; Faraday, D. Diamagnetic Anisotropy of Cyanuric Trichloride, $C_3N_3Cl_3$. *Z. Kristallogr.* **1936**, *95*, 471−471.
(31) Maginn, S. J.; Compton, R. G.; Harding, M. S.; Brennan, C. M.; Docherty, R. Evidence for Anisotropy in Chlorine Nitrogen Interactions in the Cyanuric Chloride Crystal Structure. *Tetrahedron Lett.* **1993**, *34*, 4349−4352.
(32) Pascal, R. A.; Ho, D. M. Nitrogen-Chlorine Donor-Acceptor Interactions Dominate the Structrure of Crystalline Cyanuric Chloride. *Tetrahedron Lett.* **1992**, *33*, 4707−4708.
(33) Hoppe, W.; Lenné, H. U.; Morandi, G. Strukturbestimmung von Cyanursäuretrichlorid $C_3N_3Cl_3$ mit Verwendung der diffusen Röntgenstreustrahlung zur Bestimmung der Molekülorientierungen. *Z. Kristallogr.* **1957**, *108*, 321−327.
(34) Xu, K.; Ho, D. M.; Pascal, R. A. Azaaromatic Chlorides—A Prescription for Crystal-Structures with Extensive Nitrogen-Chlorine Donor−Acceptor Interactions. *J. Am. Chem. Soc.* **1994**, *116*, 105−110.
(35) Jorgensen, W. L.; Pranata, J. Importance of Secondary Interactions in Triply Hydrogen Bonded Complexes: Guanine-Cytosine vs Uracil-2,6-diaminopyridine. *J. Am. Chem. Soc.* **1990**, *112*, 2008−2010.
(36) Lu, Y. X.; Zou, J. W.; Wang, Y. H.; Yu, Q. S. Bifurcated Halogen Bonds: An *ab Initio* Study of the Three-Center Interactions. *J. Mol. Struct. (THEOCHEM)* **2006**, *767*, 139−142.
(37) Ji, B. M.; Wang, W. Z.; Deng, D. S.; Zhang, Y. Symmetrical Bifurcated Halogen Bond: Design and Synthesis. *Cryst. Growth Des.* **2011**, *11*, 3622−3628.
(38) Jorgensen, W. L.; Jensen, K. P.; Alexandrova, A. N. Polarization Effects for Hydrogen-Bonded Complexes of Substituted Phenols with Water and Chloride Ion. *J. Chem. Theory Comput.* **2007**, *3*, 1987−1992.
(39) Schyman, P.; Jorgensen, W. L. Exploring Adsorption of Water and Ions on Carbon Surfaces Using a Polarizable Force Field. *J. Phys. Chem. Lett.* **2013**, *4*, 468−474.
(40) Chai, J. D.; Head-Gordon, M. Long-Range Corrected Hybrid Density Functionals with Damped Atom-Atom Dispersion Corrections. *Phys. Chem. Chem. Phys.* **2008**, *10*, 6615−6620.
(41) Kozuch, S.; Martin, J. M. L. Halogen Bonds: Benchmarks and Theoretical Analysis. *J. Chem. Theory Comput.* **2013**, *9*, 1918−1931.
(42) Frisch, M. J.; Trucks, G. W.; Schlegel, H. B.; Scuseria, G. E.; Robb, M. A.; Cheeseman, J. R.; Scalmani, G.; Barone, V.; Mennucci, B.; Petersson, G. A.; et al. *Gaussian 09*, Revision C.01; Gaussian: Wallingford, CT, USA, 2010.
(43) Check, C. E.; Faust, T. O.; Bailey, J. M.; Wright, B. J.; Gilbert, T. M.; Sunderlin, L. S. Addition of Polarization and Diffuse Functions to the LANL2DZ Basis Set for p-Block Elements. *J. Phys. Chem. A* **2001**, *105*, 8111−8116.
(44) Zhao, Y.; Truhlar, D. G. A New Local Density Functional for Main-Group Thermochemistry, Transition Metal Bonding, Thermochemical Kinetics, and Noncovalent Interactions. *J. Chem. Phys.* **2006**, *125*, 194101.
(45) Zhao, Y.; Truhlar, D. G. The M06 Suite of Density Functionals for Main Group Thermochemistry, Thermochemical Kinetics, Noncovalent Interactions, Excited States, and Transition Elements: Two New Functionals and Systematic Testing of Four M06-Class Functionals and 12 Other Functionals. *Theor. Chem. Acc.* **2008**, *120*, 215−241.
(46) Boys, S. F.; Bernardi, F. The Calculation of Small Molecular Interactions by the Differences of Separate Total Energies—Some Procedures with Reduced Errors. *Mol. Phys.* **1970**, *19*, 553−566.
(47) Chudzinski, M. G.; Taylor, M. S. Correlations between Computation and Experimental Thermodynamics of Halogen Bonding. *J. Org. Chem.* **2012**, *77*, 3483−3491.
(48) Glendening, E. D.; Reed, A. E.; Carpenter, J. E.; Weinhold, F. *NBO*, Version 3.1; University of Wisconsin: Madison, WI, USA, 1996.
(49) Jorgensen, W. L.; Tirado-Rives, J. Molecular Modeling of Organic and Biomolecular Systems using BOSS and MCPRO. *J. Comput. Chem.* **2005**, *26*, 1689−1700.
(50) Udier-Blagovic, M.; De Tirado, P. M.; Pearlman, S. A.; Jorgensen, W. L. Accuracy of Free Energies of Hydration Using CM1 and CM3 Atomic Charges. *J. Comput. Chem.* **2004**, *25*, 1322−1332.